6
NMR investigation of ZnO nanoparticle based drug delivery system

6.1 INTRODUCTION

Biomedical application of ZnO nanomaterials have recently been explored in the field of cancer therapy. ZnO based nanoparticles have considered as promising anticancer agents and have been used in photodynamic therapy. Specific properties and characteristics of ZnO nanomaterials, such as biocompatibility, their inherent toxicity against cancerous cells, their ability to induce intracellular ROS generation, ease of functionalization, easy synthesis make them an appealing candidate for biomedical applications. Several research groups have reported cancer chemotherapeutics based on ZnO nanoparticles or nanorods [Xie, 2016; Zhang et al., 2011; Kishwar et al., 2010; Al-Ajmi et al. 2016]. Research groups worldwide are also introducing newer synthetic routes and synthesizing hybrid nanosystems with ZnO. Drug loading, release mechanism and cytotoxicity of various ZnO_drug nanocomposites have also been studied [Cai et al., 2016; Guo et al., 2008; Muhammad et al., 2011; Tripathy et al., 2015]. Although there are number of incidences where solution state NMR experiments have been reported to understand surface functionalization and binding interaction involving ZnO nanoparticles [Rothenstein et al., 2012; Coppel et al., 2012; Coppel et al., 2012] there are a very few reports available on solid state NMR approaches applied to investigate ZnO based drug delivery systems.

Solid State Nuclear Magnetic Resonance (SS-NMR), has gained considerable attention in characterizing the structural and dynamic properties of complex functional oxides. Few recent literatures reported that a number of NMR observables, such as chemical shifts, signal broadening and intensities, relaxation parameters could be successfully investigated to characterize the structure, orientation, and dynamics of drug adsorbed onto ZnO nanoparticle surfaces. A recent review in Annual Reports on NMR spectroscopy on ^{67}Zn NMR by Huang and co-workers have mentioned the tremendous advancement in ^{67}Zn NMR that can be applied to semiconducting ZnO nanomaterials to Zn containing biomolecules [Huang et. al. 2014]. However, application of solid state NMR experiments based on multinuclear approaches to investigate ZnO based drug delivery systems especially ZnO_drug nanocomposites are still limited. Recently efforts have been made to analyze ZnO nanomaterials in terms of their surface [Peng et al., 2016], inherent impurities [Wang et al., 2015], and structural modification due to doping [Avadhut et al., 2012] by complete solid state MAS NMR methods. Moreover, slow magic angle spinning experiments have also been performed to analyze spinning side band pattern of organic ligand adsorbed on the surface. In a recent study Spataro and co-workers have reported the applicability of multinuclear ^{1}H, ^{2}H, ^{13}C, ^{15}N, ^{67}Zn and ^{17}O MAS NMR spectroscopy along with relaxation analysis to probe the structural and dynamic properties of hybrid ZnO nanomaterials. The coordination mode of an organic molecule on ZnO surface as well as the dynamics related information of organic capping molecules were evidenced [Spataro et al., 2018].

Recent advances in SS-NMR, especially the ultrafast MAS approach leads to the remarkable improvement in spectral resolution. The solid state proton NMR can easily be done with high resolution with the help of ultrafast MAS (UFMAS) technique. The use of the small rotors with diameters less than 0.75 mm leads to achieve the spinning speed up to 130 kHz .This high speed MAS efficiently averaged or suppressed the ^{1}H–^{1}H dipolar couplings which results in better spectral resolution [Zhang et al., 2017; Marchetti et al., 2012]. The application of UFMAS approach are being utilized in various biological [Bertini et al., 2010; Parthasarathy, Nishiyama, and Ishii, 2013; Reif, 2012] and chemical [Kobayashi et al., 2013; Mao et al., 2009; Zhang and Ramamoorthy, 2014; Damron et al., 2017] systems. Further, the resolution and sensitivity enhancements obtained by UFMAS based ^{1}H NMR can be used to study the insoluble non-crystalline solids which are difficult to be studied by solution NMR spectroscopy or diffraction techniques [Zhang et al., 2015]. Zhang et al have demonstrated the use of multiple-contact cross polarization (MCP) experiments under UFMAS to acquire high S/N ratio in natural-abundance ^{13}C NMR spectrum of pharmaceutical compounds [Zhang et al., 2016; Zhang et al., 2015]. They found that the signal enhancement is depends on the number of CP contacts in a scan. They have also demonstrated the utility of MCP for fast 2D $^{1}H/^{13}C$ HETCOR experiments and its applicability in characterizing polymorphic drugs and nanomaterial [Zhang et al., 2016]. The ultrafast MAS technique has also simplified the development of radiofrequency driven dipolar recoupling (RFDR) pulse sequence [Ye et al., 2014]. Zhang et al have demonstrated the utility of RFDR pulse sequence in accelerating the coherent polarization transfer among proton [Zhang et al., 2017]. They have also proposed a method for ^{1}H–^{1}H distance measurements in solids using selective excitation of specific proton under UFMAS.

With the above background, the investigation of molecular interaction of ZnO nanoparticles with anti-cancerous drug molecules becomes relevant. The present study focusses to understand the adsorption behavior of a set of anti-cancerous drugs *viz.* 5-Fluorouracil (5-FU), Doxorubicin (DOX) and Daunorubicin (DNR) on ZnO nanoparticles surfaces by employing solid state NMR measurements. In this regard, ZnO nanomaterials have been synthesized and characterized following well–established literature methods. 1D Cross Polarization (CP) and Magic Angle Spinning (MAS) based solid state NMR methods along with NMR relaxation analysis have been employed to understand surface interaction of the adsorbed drug molecules with ZnO. Further optical properties and crystallite size of the nanoparticles before and after drug loading were investigated using the UV–Visible diffuse reflectance spectroscopy (UV-DRS) and X-Ray Diffraction (XRD) measurements respectively. In brief the chapter attempts a preliminary demonstration of applicability of SS-NMR approaches for the characterization of ZnO nanoparticle based DDS.

6.2 MATERIALS AND METHODS

6.2.1 Materials

ZnO nanoparticles (ZnO NPs) were synthesized by standard precipitation method using Zinc sulfate ($ZnSO_4$) and Ammonium bicarbonate (NH_4HCO_3) as precursor. Zinc sulfate, Ammonium bicarbonate, 5-Fluorouracil (5-FU), Doxorubicin (DOX) and Daunorubicin (DNR) were purchased from Sigma-Aldrich. The chemical structures of all the drugs have been given in Figure 6.1. All chemicals were used without further purification.

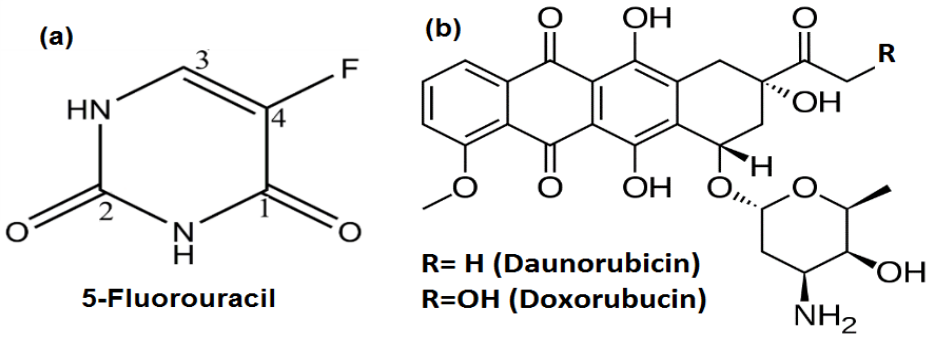

Figure 6.1 : Chemical structure of (a) 5-Fluorouracil (b) Doxorubicin and Daunorubicin

6.2.2 Preparation of ZnO nanoparticles

Several synthetic methods of preparation of ZnO nanoparticles are available in the literature. We have opted standard precipitation method for ZnO nanoparticle synthesis because of its simplicity and large-area yield at low cost.

Briefly, $ZnSO_4$ (1.5 mol/L) and NH_4HCO_3 (2.5 mol/L) were prepared in distilled water. 100 mL of $ZnSO_4$ solution was added to 126 mL of NH_4HCO_3 solution with constant stirring. The mixed solution was kept at 50°C that resulted the formation of basic zinc carbonate (BZC) slurry as white precipitate. The slurry was then filtered, washed and dried. Finally, ZnO nanoparticle was prepared by calcination of the precipitate at 500°C for 1 hour.

$$5ZnSO_4 + 10NH_4HCO_3 \rightleftharpoons Zn_5(OH)_6(CO_3)_2 \text{ (BZC)} + 5\ (NH_4)2SO_4 + 8CO_2\uparrow + 2H_2O$$

During the calcination, the BZC complex undergone decomposition and ZnO nanoparticles are obtained.

$$Zn_5(OH)_6(CO_3)_2 \rightleftharpoons 5ZnO + 2CO_2\uparrow + 3H_2O\uparrow$$

6.2.3 Preparation of ZnO_Drug Nanocomposite

Colloidal solution of ZnO nanoparticle was prepared by dispersing 0.5g ZnO nanoparticle in 20 mL water using sonication. 0.05 g of different anticancer drugs (5FU, DOX, DNR) were added to the ZnO colloidal solution with continuous stirring (1:10 ratio of drug:ZnO nanoparticles) [Hariharan et al., 2013]. The reaction mixture was kept on stirring for 48 h at room temperature under dark. The solution was then centrifuged. Drug loaded ZnO nanoparticles were dried at 50 ^{0}C for 24h.

6.2.4 Characterization of free and drug loaded ZnO nanoparticles

The synthesized ZnO nanoparticles were first characterized by FTIR, UV-DRS, XRD, ^{1}H and ^{13}C SSNMR to confirm the formation of ZnO NPs and to analyze the ZnO NPs surface. Further the changes induced in optical properties and size of NPs due to adsorption of drug molecules were investigated using the UV-DRS and XRD measurement respectively. NMR spin-lattice relaxation time measurement was also applied to understand the molecular mobility and interaction of drug on ZnO surface. The experimental details of these experiments are discussed in the following sections.

(a) Optical band gap measurement

Optical properties of the ZnO samples were measured using a UV-Vis spectrophotometer (Cary 4000) in diffuse reflectance spectral mode. UV–Vis diffuse reflectance spectra (UV-DRS) of the

free and drug loaded ZnO were recorded in the range of 200-800nm. The % reflectance obtained from the UV–DRS measurement was used for calculating the optical bandgap of the materials using the Kubelka-Munk function [Dutta and Ganguly, 2012]. The graphs of $(F(R)E)^2$ versus photon energy were plotted ($h\upsilon$) (where F(R) is the K–M function, R represents the diffuse reflectance, and $h\upsilon$ depicts the photon energy). The band gap was obtained from the intercept of the linear plot on the X-axis [Dutta and Ganguly, 2012].

(b) Crystalite size measurement

XRD patterns were obtained using Bruker D8 advance diffraction meter having Cu Kα radiation and λ = 1.54A°. The XRD data were collected in the range of (2θ) 10°–80°. Crystalline sizes were calculated from Scherrer formula [Chen et al., 2011] using the Bragg angles obtained in XRD pattern.

$$CS = \frac{0.9\lambda}{\beta \cos\theta} \text{.....(6.1)}$$

Where CS denotes the crystallite size, β represents the full width at half maximum of an hkl peak, and θ is the Bragg angle.

(c) Solid state NMR analysis

All the NMR spectra were recorded on a Bruker Ascend 500 MHz WB NMR spectrometer equipped with a solid probehead. The solid state NMR was recorded using 4mm ZrO_2 rotor spinning at MAS rate of 12 ± 0.005 kHz. All the ^{13}C spectra were acquired at natural abundance with Bruker standard 'CP' pulse sequence as discussed in Chapter 2 (section 2.6, Figure 2.13) using the ramped-amplitude (RAMP) polarization transfer [Metz et al,, 1994]. The experimental parameters used for the measurement of ^{13}C CP-MAS NMR is given in Table 6.1.

Table 6.1: Experimental parameters used for the ^{13}C CP-MAS experiment.

^{1}H hard π/2 pulse parameters	2.25 µs
^{1}H–^{13}C Contact pulse (p15)	2 ms
Spectral width (SW)	200 ppm
Data points (Td)	512
Repetition time (d1)	5.0 s
No. of scans (NS)	12000
1H decoupling sequence	spinal64 [Fung et al., 2000]

The ^{13}C longitudinal relaxation times (T_1) were measured only in case of free and ZnO surface adsorbed 5-FU (5-FU_ZnO) with 1D modification of the standard Bruker pulse sequence "cpxt1" as discussed in Chapter 2 (section 2.6.2). The relaxation delay was varied from 50 ms to 700 s with experimental time range of 8 min. to 18 h for free 5-FU while for 5-FU_ZnO sample relaxation delay was varied from 50 ms to 400 s. The number of scans used for the relaxation time measurements were 96.

6.3 RESULTS AND DISCUSSION

6.3.1 Characterization of free ZnO NPs

The FTIR spectrum of the synthesized ZnO was recorded with KBr pellet in the wavenumber range of 4000 to 400 cm^{-1} using BRUKER, Vertex 70v FT-IR spectrometer. The characteristic peak at 435 cm^{-1} as shown in Figure 6.2 (a) is the distinct stretching vibration of zinc oxide as reported in literature [Husain et al., 2014]. A broad peak at 3400 cm^{-1} was also observed possibly due to the presence of surface hydroxyl (-OH) groups on ZnO surface [Valdez et al., 2014]. We have further recorded the FTIR of ZnO NP that has undergone the blank loading process (ZnO_Blank). Beside the presence of ZnO characteristic peaks, we have observed that the small peak present at ~1500 cm^{-1} in the free ZnO NPs has enhanced significantly after undergoing the blank loading process as shown in Figure 6.2 (b). This extra peak at ~1500 cm^{-1} might be generated due to the adsorption of CO_2 on the surface of ZnO NPs [Deng, et al., 2017; Tang and Luo, 2013] which has enhanced due to the presence of dissolved CO_2 in water and 48 h exposure of the sample in open environment during the loading process.

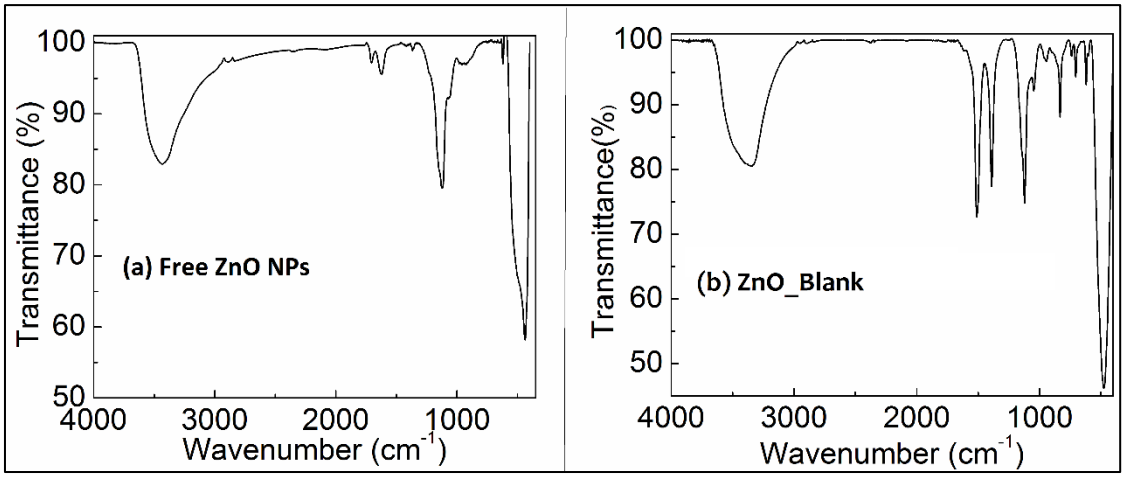

Figure 6.2 : FTIR spectrum of (a) Free ZnO NPs and (b) ZnO NPs that undergone the blank loading process (ZnO_Blank).

To further confirm the presence of –OH ions on the surface of free ZnO NPs, we have recorded the ^{1}H solid state NMR of ZnO NPs using the Bruker standard 'onepulse' sequence. Solid state ^{1}H NMR of ZnO NPs also showed a broad ^{1}H peak at 7.5 ppm confirming the presence of –OH ions on ZnO surface as shown in Figure 6.3.

^{13}C CP-MAS NMR of ZnO NPs does not show any carbon signal as shown in Figure 6.4 (a) which suggest that ZnO NPs are free from any impurity while the ZnO_Blank sample has exhibited a sharp ^{13}C signal at ~165 ppm with a line broadening of ~75 Hz as shown in Figure 6.4 (b). This ^{13}C signal at ~165 ppm further confirms the adsorption of CO_2 (trapped CO_2) on ZnO NPs surface during the loading process.

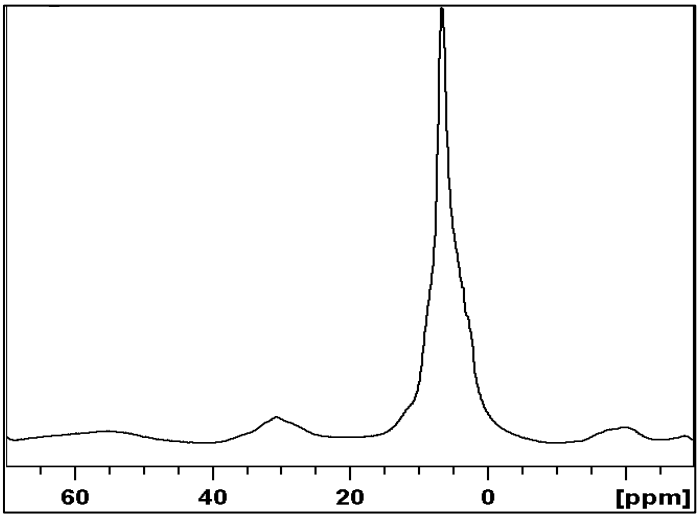

Figure 6.3 : Solid state ^{1}H NMR spectra of Free ZnO NPs at MAS frequency of 12 KHz.

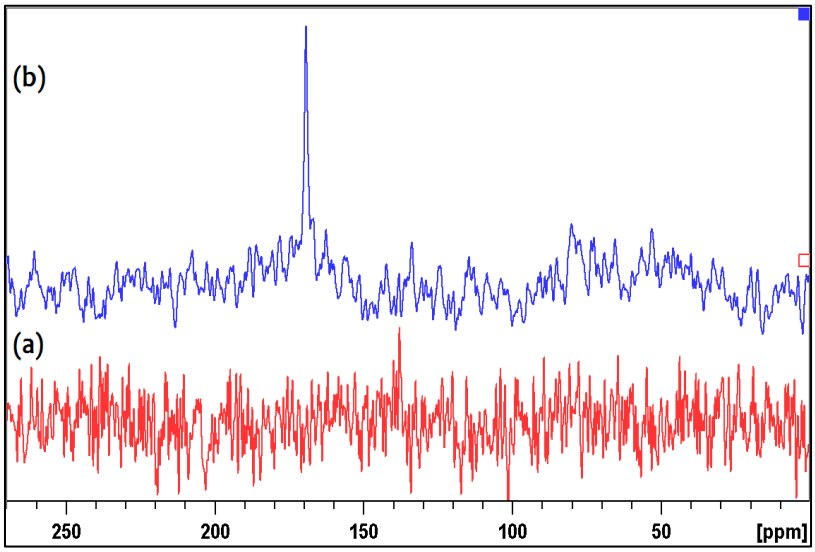

Figure 6.4 : ^{13}C CPMAS NMR of (a) Free ZnO NPs and (b) ZnO_Blank recorded at MAS frequency 12 kHz.

6.3.2 UV–DRS analysis of free and drug loaded ZnO NPs

UV–Vis diffuse reflectance spectra of the free and drug loaded ZnO nanoparticles and corresponding optical band gap are shown in Figure 6.5 (a). ZnO nanoparticles showed an absorption edge at ~400 nm. The intrinsic band-gap energy correspond to this reflectance was determined as 3.21 eV as shown in Figure 6.5 (b) which was in agreement with the literature [Velusamy and Lakshmi, 2017]. The lower band gap for ZnO nanoparticles compared to the bulk ZnO (3.3 eV) could be reasoned out as the agglomeration of the nanoparticles as discussed in previous literature [Indubala et al., 2018]. For drug loaded ZnO samples, the band gaps were estimated as shown in Figure 6.5 (b) and Table 6.2. Decrease of % reflectance in UV-DRS of drug loaded ZnO revealed the modification of ZnO surface due to the adsorption of drug. The higher reduction of % reflectance in case of doxorubicin and daunorubicin could be attributed to the presence of greater number of chromophores in these drugs compared to 5-fluorouracil. Further, the lower band gap of drug loaded ZnO nanoparticles could be attributed to the higher

concentration of the carrier in ZnO after loading of drug. The higher electron concentration in the valence band leads to the decrement of energy barrier for electronic transition between conduction band and valance band. Therefore, the drug loaded ZnO can be easily excited and the number of electron–hole pairs generated is in large extent. Further, the higher photocatalytic activity can be seen in such ZnO_drug samples [Li et al., 2014].

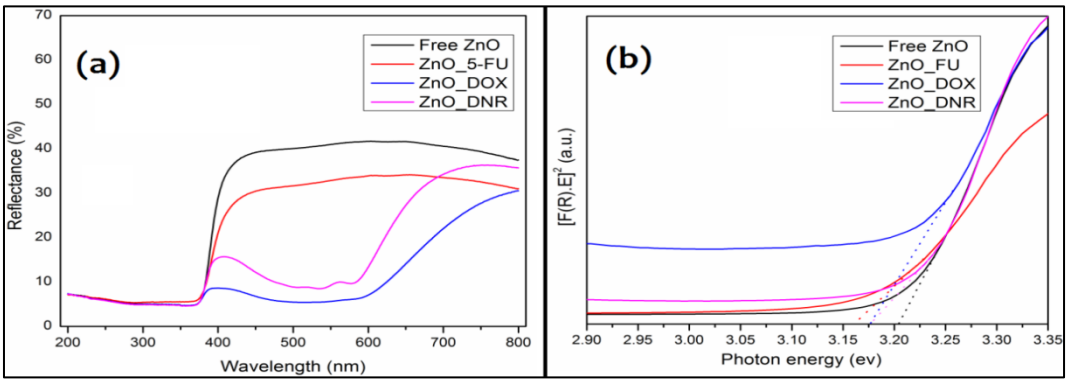

FIGURE 6.5 : (a) UV-Vis. diffuse reflectance spectra and (b) plot of Kubelka-Munk function to estimate bandgap of free and drug loaded ZnO NPs.

TABLE 6.2 : Optical Band gap measured for free and drug loaded ZnO NPs using the Kubelka-Munk function.

Sample	Free ZnO	ZnO_5-FU	ZnO_DOX	ZnO_DNR
Band Gap (eV)	3.210	3.165	3.175	3.175

6.3.3 X-ray Diffraction (XRD) analysis

XRD results provide us the characteristic diffraction pattern of the drug loaded ZnO NPs. Figure 6.6 shows the XRD patterns of the free and drug loaded ZnO NPs. The pure ZnO sample showed the characteristic diffraction patterns of ZnO that are similar to the standard XRD patterns of bulk ZnO crystals having wurtzite structure [Baruah and Dutta, 2009; Khan, et al., 2011]. The XRD patterns of ZnO samples after the drug loading are similar to the pure ZnO, which suggests that the adsorption of drug molecule does not affect the crystal structure of the ZnO nanoparticles and it remains intact after the drug loading.

Further, the average crystallite sizes of the free and drug loaded ZnO samples were estimated from line broadening of the XRD peaks using Scherrer's formula. The crystallite size for free and drug loaded ZnO nanoparticles are shown in Table 6.3. The crystallite size of pure ZnO is 14.22 nm, whereas it increases to 23.58, 31.05 and 26.26 nm after loading of 5FU, DOX and DNR respectively. These findings confirm the adsorption of drug molecules on the surface of ZnO. The crystallite sizes of drug loaded ZnO nanoparticles are still smaller than 50 nm, which is under the prescribed limit and can be used for targeted delivery [Tran et al., 2017].

Table 6.3 : Crystallite size measured for free and drug loaded ZnO nanoparticles using the Scherrer's formula.

Sample	Free ZnO	ZnO_5-FU	ZnO_DOX	ZnO_DNR
Crystallite Size (nm)	14.22	23.58	31.05	26.26

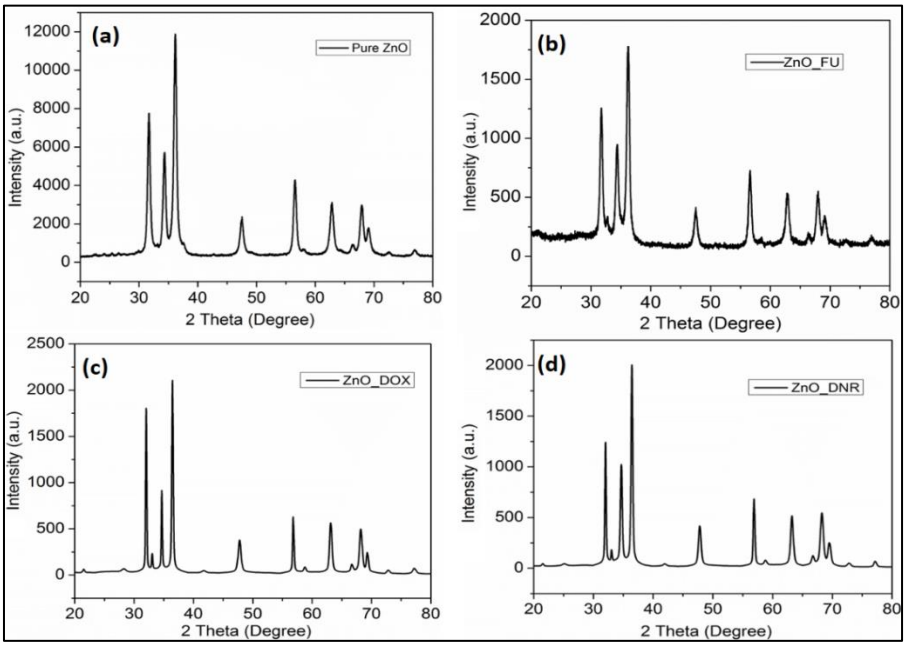

FIGURE 6.6 X-Ray diffraction pattern of (a) free ZnO nanoparticle (b) ZnO_5-FU (c) ZnO_DOX and (d) ZnO_DNR.

6.3.4 ^{13}C CP-MAS NMR

Solid state ^{13}C CP-MAS NMR experiments have been employed for the drugs (5-FU, DOX and DNR) in free and ZnO adsorbed samples to understand the interaction of drugs with ZnO NPs surface. Figure 6.7, 6.8 and 6.9 represent the ^{13}C CP-MAS NMR of free and ZnO surface adsorbed 5-FU, DOX and DNR respectively. The spectra were recorded with 12 k number of scans amounting to an experimental time of 12 h.

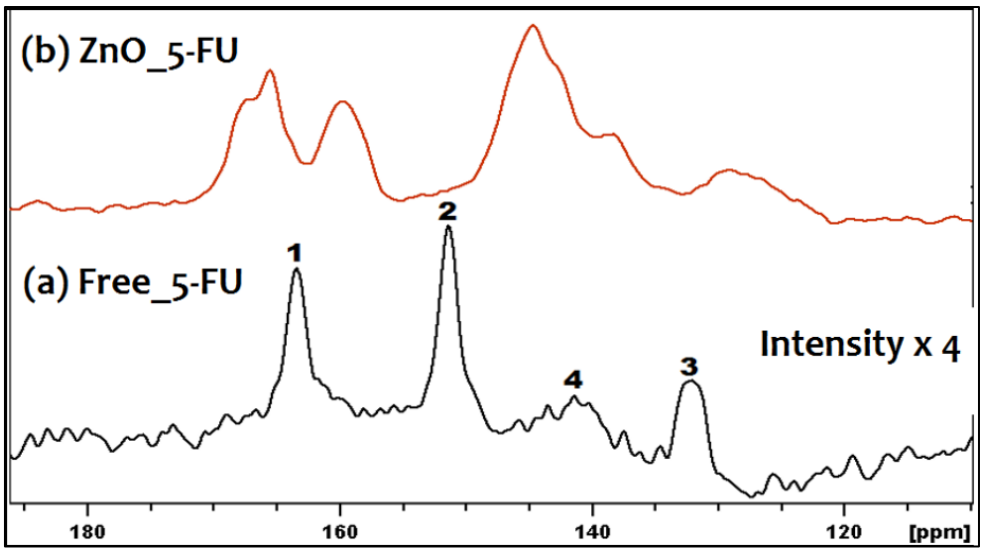

Figure 6.7 : Stack plot of ^{13}C CP-MAS NMR spectra of (a) Free 5-FU and (b) ZnO_5-FU sample at MAS frequency of 12 kHz.

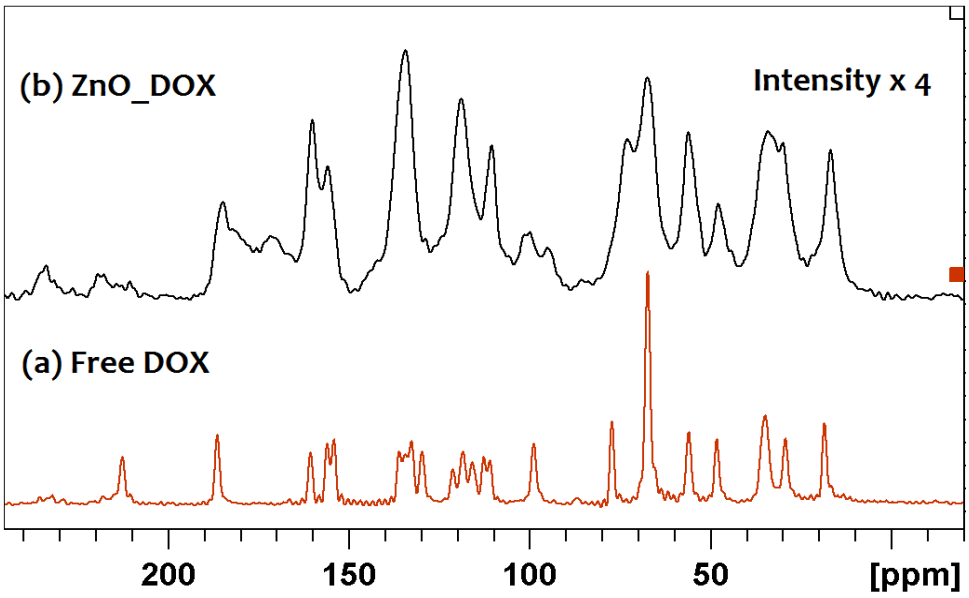

Figure 6.8 : Stack plot of ^{13}C CP-MAS NMR spectra of (a) Free DOX and (b) ZnO_DOX sample at MAS frequency of 12 kHz.

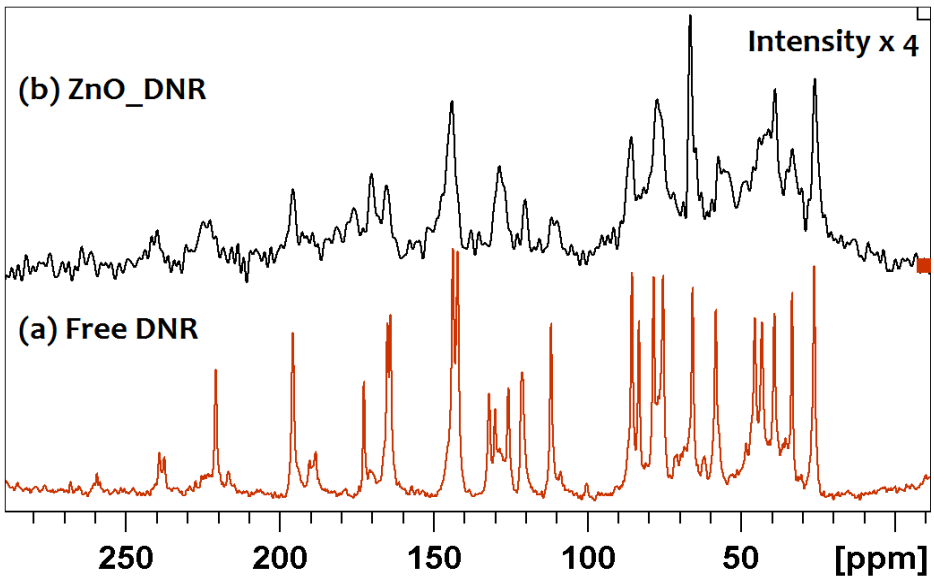

Figure 6.9 : Stack plot of ^{13}C CP-MAS NMR spectra of (a) Free DNR and (b) ZnO_DNR sample at MAS 12 kHz.

Changes in NMR signal intensities and line broadening have been observed for all the samples after the adsorption on ZnO surface. However, the ZnO_5-FU sample showed magnificent signal enhancement besides line broadening and changes in chemical shifts positions compared to ZnO_DOX and ZnO_DNR. The signal to noise ratio (S/N) calculated for the carbonyl carbon (—C=O) has increased by ~81% in ZnO_5-FU compared to the free 5-FU while S/N ratio has been decreased by ~49% and ~88% for ZnO_DOX and ZnO_DNR samples respectively compared to their free drug forms. It is also worth mentioning here that the ^{13}C CP-MAS NMR of free drugs have been recorded in their pure form as such while the ZnO adsorbed drug samples are having 1:10 ratio of drug:ZnO. Therefore the intensities of ^{13}C signals were expected to be decreased in drug loaded ZnO samples. The remarkable enhancement in the ^{13}C signal intensities in ZnO_5-FU sample could be explained as the possibility of cross polarization from the protons of the ZnO surface hydroxyl (−OH) groups to the carbons of 5-FU. Table 6.4 has summarized the changes in chemical shifts positions and line broadening in ZnO_5-FU

compared to the free 5-FU. The changes in these NMR parameters suggest that the chemical environment and mobility experienced by 5-FU is significantly modified after the adsorption on ZnO surface.

Table 6.4 : ^{13}C Chemical shifts and linewidths measured for free 5-FU and ZnO_5-FU sample at 300K using CP-MAS experiment.

Carbon	Free 5-FU		ZnO_5-FU		
	Chemical shift (δ_{ppm})	Linewidth (Hz)	Chemical shift (δ_{ppm})	$\Delta\delta_{ppm}$	Linewidth (Hz)
C-1	163 ± 0.7	147 ± 2.3	166 ± 0.9	3.0 ± 1.1	501 ± 2.9
C-2	151 ± 1.1	125 ± 1.6	159 ± 0.8	8.0 ± 1.4	541 ± 1.7
C-3	132 ± 0.4	234 ± 0.9	128 ± 1.2	-4.0 ± 1.3	621 ± 3.2
C-4	140 ± 1.2	309 ± 2.7	144 ± 0.6	2.0 ± 1.3	901 ± 2.4

The highest enhancement in linewidth (592.48 Hz) and peak intensity were observed for the C-4 of 5-FU having –F atom on it. Therefore one may conclude that the 5-FU was possibly adsorbed on the ZnO surface through the fluorinated end. Strong electrostatic or H-bonding attraction between the surface –OH group of ZnO and –F atom of the 5-FU might be the reason for this interaction. Further this strong interaction leads to the rigid structure of 5-FU on ZnO surface offering a very efficient polarization transfer from the proton of ZnO surface –OH group to the carbons of 5-FU. We further, investigated the spin-lattice relaxation time of free 5-FU and ZnO_5-FU samples to unravel the dynamic properties of 5-FU on ZnO NPs surface

6.3.5 ^{13}C spin-lattice relaxation time measurement

^{13}C spin lattice relaxation times (T_1) were measured using the 'Torchia' method as discussed in Chapter 2 (section 2.6.2). It is well known from the literature that the ^{13}C T_1 in solid states are considerably longer and ranges from several seconds to few hours. Similar trend for free 5-FU has been observed in our case; the free 5-FU showed very long ^{13}C T_1 values (~400 s) as shown in Table 6.5. We have chosen C-2 carbon (151.39 ppm) of 5-FU to measure the T_1 of free 5-FU and ZnO_5-FU since it gives a well resolved and significantly intense peak in both the samples. Also, the C-3 and C-4 peaks exhibit very less intensity in free 5-FU while the C-1 peak has merged with the adsorbed CO_2 peak (~167 ppm) in ZnO_5-FU sample. It has been observed that the ^{13}C T_1 value of 5-FU loaded on ZnO NPs have considerably decreased compared to the free 5-FU. Table 6.5 has summarized the ^{13}C T_1 value of 5-FU C-2 in free 5-FU and ZnO_5-FU sample.

Table 6.5 : ^{13}C spin-lattice relaxation time (T_1) measured for 5-FU C-2 in free 5-FU and ZnO_5-FU sample using the Torchia method.

Sample	Free 5-FU	ZnO_5-FU
^{13}C T_1 for C-2 of 5-FU	426 ± 5.1 s	89 ± 3.2 s

^{67}Zn and ^{17}O are quadrupolar nuclei with quadupolar moment of 15.0×10^{-30} m^2 and -2.6×10^{-30} m^2 respectively [Stone, 2005]. The possible quadrupolar interaction of these nuclei with ^{13}C leading to faster relaxation could be the reason for observed shorter T_1. Besides, the higher

quadupolar moment, the natural abundance of ^{67}Zn (4.11%) is also very high compared to the ^{17}O (0.037%). Therefore the quadrupolar interaction from ^{67}Zn would be the dominant factor for this shorter T_1 in ZnO_5-FU sample. Further this shorter T_1 value confirms the rigid structure of 5-FU on ZnO surface leading to the strong quadrapolar contribution from ^{67}Zn. This variation in T_1 value also suggests a notable change of the local motions of the 5-FU when it is interacting with the ZnO surface.

6.4 Conclusion

ZnO nanoparticle based drug delivery systems with different anticancer drugs have been developed. The optical band gap investigations with UV-DRS and crystallite size determination with XRD have been carried out in order to understand the changes involved in such drug loaded ZnO DDSs. Enhanced photo-catalytic activity and crystallite size due to adsorption of drug on ZnO nanoparticles are noticeable effect as seen from our results. FTIR and ^{1}H solid state MAS NMR data confirmed the presence of adsorbed hydroxyls (–OH) groups on bare ZnO surface. Further, significant line broadening and changes in chemical shift positions were observed in ^{13}C CP-MAS NMR spectra of ZnO_5-FU that supports the UV-DRS data of surface adsorption. Remarkable enhancement of ^{13}C signal intensity in case of 5-FU loaded ZnO sample compared to free 5-FU indicated strong adsorption of the 5-FU resulting improved polarization transfer from surface hydroxyl groups of ZnO surface. The ^{13}C NMR data also indicated possible mode of adsorption. The relaxation measurements confirms the rigid structure and changes in the dynamic character of 5-FU on ZnO surface. This study primarily demonstrates the efficiency and pertinence of SS-NMR spectroscopy to obtain the detailed structural and dynamic information of nanoparticles based DDSs.

…